American Journal of Transplantation 24 (2024) 1414–1426

Contents lists available at ScienceDirect

American Journal of Transplantation

journal homepage: www.amjtransplant.org

Original Article

Redefining the molecular rejection states in 3230 heart transplant biopsies: Relationships to parenchymal injury and graft survival

Philip F. Halloran [1,*], Katelynn Madill-Thomsen [1], Arezu Z. Aliabadi-Zuckermann [2], Martin Cadeiras [3], Marisa G. Crespo-Leiro [4], Eugene C. Depasquale [3], Mario Deng [3], Johannes Gökler [2], Shelley Hall [5], Aayla Jamil [5], Daniel H. Kim [1], Jon Kobashigawa [6], Peter Macdonald [7], Vojtech Melenovsky [8], Jignesh Patel [6], Luciano Potena [9], Keyur Shah [10], Josef Stehlik [11], Andreas Zuckermann [2]

[1] *Department of Medicine, University of Alberta, Edmonton, Alberta, Canada*
[2] *Department of Cardiac Surgery, Medical University of Vienna, Vienna, Austria*
[3] *Ronald Reagan UCLA Medical Center, Los Angeles, California, USA*
[4] *Advanced Heart Failure and Heart Transplant Unit, Complexo Hospitalario Universitario A Coruña, A Coruña, Spain*
[5] *Baylor Scott & White Health, Dallas, Texas, USA*
[6] *Smidt Heart Institute, Cedars-Sinai Medical Center, Los Angeles, California, USA*
[7] *The Victor Chang Cardiac Research Institute, Sydney, Australia*
[8] *Department of Cardiology, Institute for Clinical and Experimental Medicine (IKEM), Prague, Czech Republic*
[9] *Heart Failure and Transplant Unit, IRCCS Azienda Ospedaliero-Universitaria di Bologna, Bologna, Italy*
[10] *Department of Cardiology, Virginia Commonwealth University, Richmond, Virginia, USA*
[11] *Department of Medicine, University of Utah, Salt Lake City, Utah, USA*

ARTICLE INFO

Keywords:
heart transplant biopsy
biopsy

ABSTRACT

The first-generation Molecular Microscope (MMDx) system for heart transplant endomyocardial biopsies used expression of rejection-associated transcripts (RATs) to diagnose not only T cell–mediated rejection (TCMR) and antibody-mediated rejection (ABMR) but also

Abbreviations: AA, archetypal analysis; ABMR, antibody-mediated rejection; AMATs, alternative macrophage activation transcripts; ATAGC, Alberta Transplant Applied Genomics Centre; AUC, area under the curve; BAT, B cell-associated transcripts; CAV, cardiac allograft vasculopathy; cIRIT, cardiac injury and repair transcripts; DAMP, damage-associated molecular pattern transcripts; DSA, Donor-specific antibody; DSAST, DSA-selective transcripts; EABMR, Early-stage ABMR; EMB, endomyocardial biopsy; FABMR, Fully-developed ABMR; gmlnet, a package that fits a generalized linear model via penalized maximum likelihood; GRIT, Gamma interferon and rejection induced transcripts; HT, heart parenchymal transcripts; HT1, heart parenchymal transcripts set 1; HT2, heart parenchymal transcripts set 2; IGT, immunoglobulin transcripts; INTERHEART, Diagnostic and Therapeutic Applications of Microarrays in Heart Transplantation, a Multicenter Study, (ClinicalTrials.gov Identifier: NCT02670408); Injury archetype, archetypal model for assessing cardiac injury; IRRAT, injury-and-repair transcripts; IRITD3, injury-repair induced transcripts day 3; IRITD5, injury-repair induced transcripts day 5; KCL, Kashi Clinical Laboratories; LVEF, left ventricular ejection fraction; LoLVEFProb, Low LVEF probability classifier; MMDx, Molecular Microscope® Diagnostic System; NKB, natural killer cell burden; NR, No rejection; pABMR, Probable ABMR; PBTs, pathogenesis-based transcript sets; PCA, principal component analysis; PC1, principal component 1; PC2, principal component 2; PC3, principal component 3; pTCMR, Probable TCMR; QCAT, Quantitative cytotoxic T cell-associated transcripts; QCMAT, Quantitative constitutive macrophage-associated transcripts; RATs, rejection-associated transcripts; TCMR, T cell-mediated rejection; TCMR1, TCMR type 1; TCMR2, TCMR type 2; TxBx, Time of biopsy post-transplant; UMAP, Uniform manifold approximation and projection.

* Corresponding author. Philip F Halloran, Alberta Transplant Applied Genomics Centre, #250 Heritage Medical Research Centre, University of Alberta, Edmonton, AB T6G 2S2, Canada.
E-mail address: phallora@ualberta.ca (P.F. Halloran).

https://doi.org/10.1016/j.ajt.2024.03.031
Received 13 December 2023; Received in revised form 15 March 2024; Accepted 20 March 2024
Available online 26 March 2024

gene expression
rejection
injury
graft survival

acute injury. However, the ideal system should detect rejection without being influenced by injury, to permit analysis of the relationship between rejection and parenchymal injury. To achieve this, we developed a new rejection classification in an expanded cohort of 3230 biopsies: 1641 from INTERHEART (ClinicalTrials.gov NCT02670408), plus 1589 service biopsies added to improve the power of the machine learning algorithms. The new system used 6 rejection classifiers instead of RATs and generated 7 rejection archetypes: No rejection, 48%; Minor, 24%; TCMR1, 2.3%; TCMR2, 2.7%; TCMR/mixed, 2.7%; early-stage ABMR, 3.9%; and fully developed ABMR, 16%. Using rejection classifiers eliminated cross-reactions with acute injury, permitting separate assessment of rejection and injury. TCMR was associated with severe-recent injury and late atrophy-fibrosis and rarely had normal parenchyma. ABMR was better tolerated, seldom producing severe injury, but in later biopsies was often associated with atrophy-fibrosis, indicating long-term risk. Graft survival and left ventricular ejection fraction were reduced not only in hearts with TCMR but also in hearts with severe-recent injury and atrophy-fibrosis, even without rejection.

1. Introduction

Heart transplant survival is currently estimated to be 50% at 10 years posttransplant, underscoring the need for innovations to improve management.[1,2] Molecular biopsy analysis presents an opportunity to identify rejection and injury to support new management approaches and enhance clinical trials. With this goal in mind, we developed the Molecular Microscope Diagnostic System (MMDx)[3-6] for heart transplant endomyocardial biopsies (EMBs) in the INTERHEART study (ClinicalTrials.gov NCT02670408), aiming to assess molecular T cell–mediated rejection (TCMR) and antibody-mediated rejection (ABMR) and to understand the molecular changes associated with heart injury. The first-generation MMDx measured expression of rejection-associated transcripts (RATs)[3-9] in EMBs using genome-wide microarrays and applied an ensemble of machine learning algorithms to diagnose TCMR and ABMR. However, in addition to detecting rejection, the first-generation RAT-based MMDx system also detected acute parenchymal injury because some RATs are induced by injury as well as by rejection.[4] This is a problem because rejection and parenchymal injury can both be present, and shows that it would be advantageous to be able to assess both the extent of rejection and the extent of injury separately.

This study aimed to expand the reference set to improve the power of the machine learning algorithms; develop a new MMDx system for assessing rejection that separated rejection from parenchymal injury; and use this new system to define the relationship between the new rejection classes and the parenchymal injury states. Instead of using kidney-derived RATs to define rejection, we used 6 kidney-derived rejection classifier scores as input to the archetypal classification. Based on our experience in kidney transplants where classifiers diagnose rejection without cross-reactions with injury,[10] we hypothesized that rejection classifiers eliminate the cross-reactions between rejection and acute injury observed with the RAT-based MMDx-Heart system.[9] This would allow us to compare the pure rejection state of each biopsy to its parenchymal injury state defined by heart injury archetype system.[5] We have experience using molecular classifiers for heart transplant biopsies because we developed classifiers to identify the molecular features associated with reduced left ventricular ejection fraction (LVEF) and impaired graft survival.[9] For a glossary of abbreviations, see Supplementary Table 1.

2. Materials and methods

2.1. Experimental design

A flowchart describing the molecular diagnostic classes in this article and a consort diagram are shown in Figure 1.

2.2. Patient and biopsy population

In total, 3230 standard-of-care EMBs were collected for clinical indications or for protocol/surveillance from consenting patients by participating INTERHEART (ClinicalTrials.gov: NCT02670408) investigators at 13 centers throughout Canada, the United States, Australia, and Europe (Supplementary Table 2). Some INTERHEART biopsies were previously described.[5,8,9]

Details of the INTERHEART and service biopsy populations are shown in Supplementary Table 3. INTERHEART biopsies (N=1641) were collected from consented patients as approved by ethics review boards at each center and processed at the Alberta Transplant Applied Genomics Center (ATAGC) . To these, we added 1589 service biopsies from the Kashi Clinical Laboratories (KCL)[9] to increase the number of biopsies available for the archetypal analyses (Fig. 1A and Supplementary Table 3). Biopsy-processing methods were standardized between ATAGC and KCL.

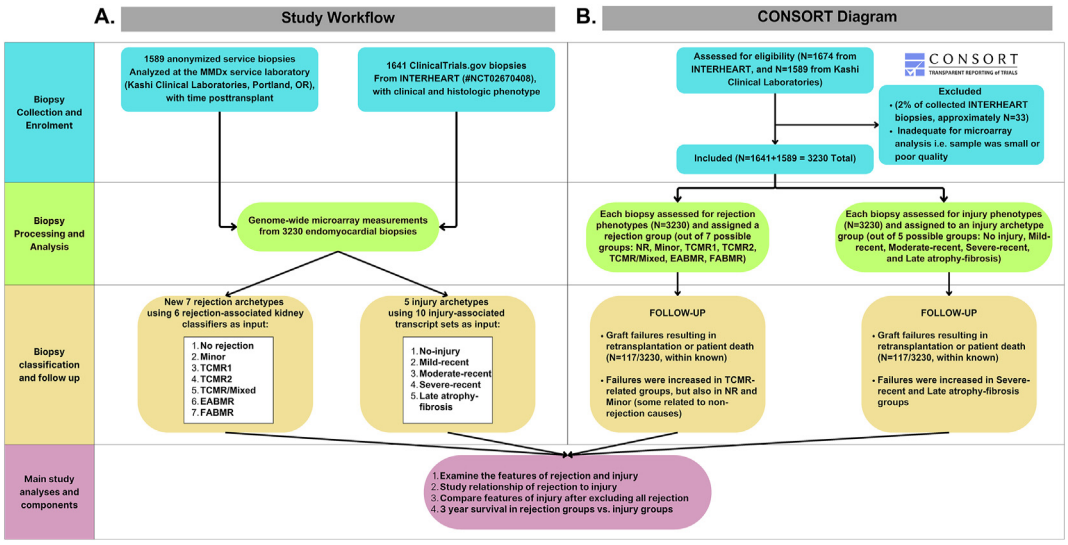

Figure 1. (A) Study design and (B) CONSORT diagram showing biopsy inclusion for the INTERHEART (N = 3230) data set. ABMR, antibody-mediated rejection; EABMR, early-stage antibody-mediated rejection; FABMR, fully developed antibody-mediated rejection; NR, No rejection; TCMR, T cell–mediated rejection.

Histologic assessment per International Society for Heart and Lung Transplantation guidelines[11-13] was available for 1435 of the 1641 INTERHEART biopsies.[4,6,9,14] To compare MMDx rejection archetypes (Table 1) to histology signouts from the local centers, we grouped the signouts as No rejection (NR), TCMR, Mixed, probable TCMR, probable ABMR, and ABMR, as previously described[6] (detailed in Table 2 footnote). The follow-up status postbiopsy was recorded as alive with functioning graft at the last follow-up (dated); failed (record date)—dead or retransplanted; or unknown (eg, lost to follow-up at the center that performed the biopsy). Follow-up information was not available for the service biopsies processed by KCL because these patients had not consented for their medical records to be accessed. Both surveillance/protocol and indication biopsies were included as a sample of the biopsies from the prevalent heart transplant population.

2.3. Microarray analysis

Biopsies for MMDx were placed in RNAlater and shipped to ATAGC.[15] MMDx measured gene expression using genome-wide microarrays and interpreted the results by machine learning.[16] RNA was labeled as previously described[4,6,7] and hybridized to PrimeView microarrays (Affymetrix). CEL files are available on Gene Expression Omnibus (GSE262742). Differential expression was by Bayesian *t* test using the "limma" package[17] in R.[18] MMDx reports were signed out, as previously described.[4,6] Molecular and histology analyses were blinded to one another. MMDx excluded approximately 2% of submitted biopsies owing to inadequacy for molecular examination.

2.4. Dimensionality reduction, clustering, and data visualization

Principal component analysis (PCA) was used to simplify the analysis of high-dimensionality data sets.[4,6] Archetypal analysis defined a specified number (n) of idealized archetypes, then assigned each biopsy n scores (summing to 1) that reflect their similarity to each archetype.[4,6] The highest score for each biopsy defined its archetype group membership.

2.5. Developing a new rejection archetype model

Previous rejection archetype models[8] using RATs as input also detected an injury state. To assess rejection independently of injury, we generated a new model that used 6 published classifiers, previously trained on diagnoses and rejection-specific lesions of ABMR and TCMR in a population of 1208 kidney transplant biopsies: the $ABMR_{Prob}$, ptc $> 0_{Prob}$, g $> 0_{Prob}$, $TCMR_{Prob}$, t $> 1_{Prob}$, and i $> 1_{Prob}$ classifiers[10] (Supplementary Table 4). As was the case for using kidney-derived RATs, the use of kidney-derived rejection classifiers in a population of heart transplants is possible because the gene expression states are conserved between heart and kidney.[14] The classifiers were trained on the molecular features associated with histologic ABMR (diagnosis, ptc-lesions, or g-lesions) and TCMR (diagnosis, t-lesions, or i-lesions). Thus, the classifiers are detecting the molecular ABMR or TCMR states, which are highly similar between kidney and heart transplants,[14] not the histologic features themselves. When using the kidney classifiers, the hearts were normalized as kidneys using the kidney reference set and robust multiarray averaging. For everything else, they were normalized as hearts using the same methods. The input for rejection PCA and archetypal analysis was a 3230 (biopsy) $\times$ 6 (rejection classifier score) data set, using "FactoMineR"[19] and "archetypes"[20] packages.

2.6. Transcript sets

Transcript sets (Supplementary Table 5) were previously annotated in cell lines, experimental models, and human transplant

Table 1
Features of the 7 rejection archetype groups in 3230 biopsies.

Biopsy groups	Feature	No rejection	Minor	TCMR1	TCMR2	TCMR/mixed	Early-stage ABMR	Fully developed ABMR
	n (%)	1564 (48.4)	777 (24.1)	75 (2.3)	88 (2.7)	88 (2.7)	127 (3.9)	511 (16)
	Days posttransplant (median)	189[a]	356	360	660	938	266	1328[b,c]
	Days posttransplant (mean)	1012[a]	1157	1077	1183	1497	1116	1708[b,c]
TCMR-related	Cytotoxic T-cell transcripts (QCATs)	0.75[a]	1.06	2.91[b,c]	2.21	2.57	1.77	1.78
All rejection	Interferon gamma-inducible transcripts (GRIT1)	0.79[a]	1.09	2.24[b,c]	1.80	2.03	1.53	1.63
ABMR-related	DSA-selective transcripts (DSASTs)	0.78[a]	0.95	0.92	0.83	1.27	1.06	1.38[b,c]
	Natural killer cell burden (NKB)	0.89[a]	1.12	1.41	1.04	1.75	1.35	1.91[b,c]
	DSA positive status	0.32	0.42	0.27[a,b]	0.47	0.78[b,c]	0.53	0.70
Macrophage transcripts (QCMATs)		0.78[a]	0.89	2.01[b,c]	1.54	1.71	1.23	1.21
Normal heart transcripts (HT)		0.83[c]	0.82	0.44[a,b]	0.58	0.53	0.72	0.71
Recent injury-induced transcripts (cIRIT)		0.84 [a]	0.85	1.21[b,c]	1.06	1.11	0.97	0.97
Function	Mean LVEF	61	63[c]	54	45[a,b]	56	61	61
	Fraction with low LVEF $\leq$ 55	0.19	0.16[a]	0.44	0.82[b,c]	0.41	0.26	0.20
	Classifier score $LoLVEF_{Prob}$	0.17	0.16[a]	0.45	0.48[b,c]	0.41	0.23	0.21

ABMR, antibody-mediated rejection; LVEF, left ventricular ejection fraction; $LoLVEF_{Prob}$, low left ventricular ejection fraction–previously published; TCMR, T cell–mediated rejection.

[a] The lowest per row.

[b] The highest per row.

[c] The most abnormal (compared with the no rejection group) per row.

Table 2
Relating the histology rejection diagnoses to the molecular rejection archetypes in 1435 biopsies.

Histologic rejection classes[a]	Molecular rejection archetypes					Sum of rows
	No rejection	Minor (mild ABMR and/or TCMR molecular changes)	TCMR (1+2)	TCMR/Mixed	ABMR (Early-stage and Fully developed)	
No Rejection	454[b]	121	11	3	50	639
Possible TCMR	213	117[a]	16	10	70	426
Possible ABMR	39	45[b]	11	12	48	155
TCMR	40	29	25[b]	8	19	121
Mixed	3	4	**7**	1[b]	2	17
ABMR	14	23	0	9	31[b]	77
Sum of columns	763	339	70	43	220	1435

ABMR, antibody-mediated rejection; TCMR, T cell–mediated rejection.

[a] To compare histologic rejection diagnoses with molecular rejection archetypes, histologic diagnoses from each center were be simplified as follows: pAMR0 = no ABMR; pAMR1, pAMR1I+, pAMR1H+ = possible ABMR (pABMR); pAMR2 = pAMR3 ABMR; TCMR0R = no TCMR; TCMR1R = possible TCMR (pTCMR); TCMR2R, TCMR3R = TCMR.

[b] Histology-molecular agreement.

biopsies (https://www.ualberta.ca/medicine/institutes-centres-groups/atagc/research/gene-lists). Transcript set scores are the means of fold changes compared with controls (371 biopsies with no molecular rejection >30 days posttransplant), calculated using the original $\log_2$ raw data.

2.7. Updating the 5 archetype model of heart injury

The previous injury 5 archetype model[5] was rederived using the injury pathogenesis-based transcript sets described in Supplementary Table 5.

2.8. Low left ventricular ejection fraction and survival

For survival, multivariable Cox regression was performed assessing 3-year death-censored survival using "cph" from the R package "rms."[21] The predictor variables were heavily right-skewed and therefore log-transformed. Graft failures were recorded as 1 (graft failure) versus 0 (graft still functioning at the time of follow-up) by the local center per standard of care. Low left ventricular ejection fraction was defined as ≤55. The $\text{LoLVEF}_{\text{Prob}}$ classifier was previously published.[9]

2.9. Relationships to time posttransplant

Probability of archetype assignments versus time posttransplant used logistic regression and the 'rcs'[22] function in R.

3. Results

3.1. Study population and demographics

The clinical and histologic demographics of the 1641 INTERHEART clinical trials biopsies (Supplementary Table 3) were similar to those previously described.[9] We added 1589 anonymized service biopsies from KCL, creating an expanded 3230 biopsy cohort.

3.2. Deriving new rejection archetypes using rejection classifiers

All 3230 biopsies were given scores reflecting molecular ABMR and/or TCMR using 6 rejection classifiers, including 3 detecting TCMR and 3 detecting ABMR. In kidney transplants, these classifiers identify rejection states without cross-reacting with acute injury.[10] The 6 classifier scores were used to distribute the biopsies in PCA (Fig. 2), showing the vectors for each classifier. Figure 2A shows the vectors in PC2 vs PC1, and Figure 2B shows PC2 vs PC3.

Figure 2C, D shows the biopsies distributed in PCA and colored by archetype assignments: 1564 NR (48%), 777 Minor (24%, a lower percentage than in previous analyses[8]), 75 TCMR1 (2.3%), 88 TCMR2 (2.7%), 88 TCMR/Mixed (2.7%), 127 early-stage ABMR (EABMR) (3.9%), and 511 FABMR (15.8%). Thus, 251 biopsies (8%) had TCMR (including mixed) and 638 biopsies (20%) had ABMR. There was no acute injury archetype in the classifier-based rejection archetypes. Similar to the earlier rejection analyses, PC1 reflected all rejection and PC2 separated ABMR (positive) from TCMR (negative). However, although PC3 in the RAT model detected early injury,[8] PC3 in the new classifier model separated TCMR1 from TCMR2. This validates our hypothesis that rejection classifiers would eliminate the cross-reaction with acute injury that occurred with RATs and permit separate assessment of the rejection state and injury state in each biopsy.

We also visualized the rejection archetypes using uniform manifold approximation and projection (UMAP), compressing all rejection-related variance to 2 dimensions (Fig. 2E).

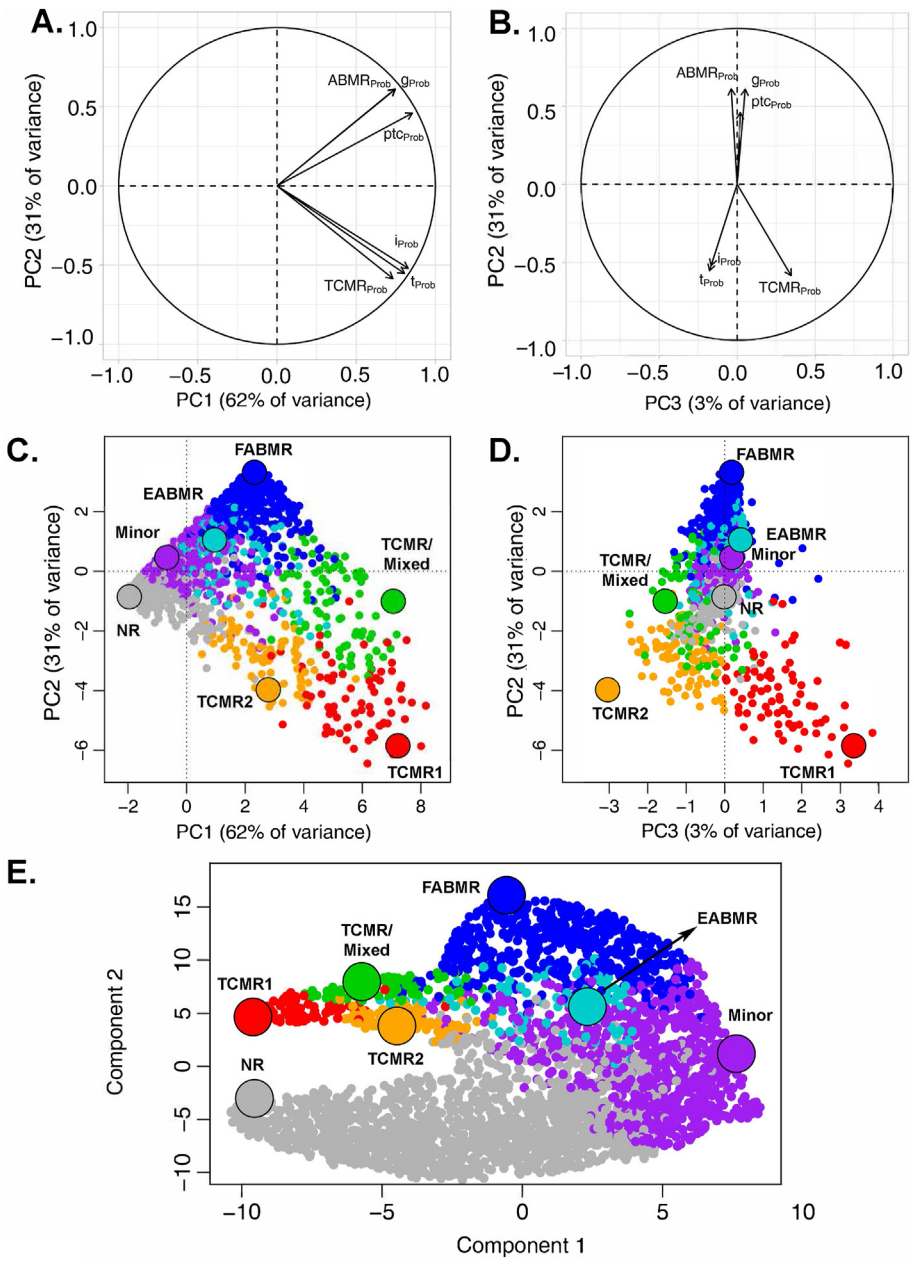

Figure 2. Principal component analysis (PCA), archetypal analysis, and uniform manifold approximation and projection (UMAP) using 6 kidney-derived rejection classifiers in the 3230 heart transplant biopsy population. The correlations between the 6 kidney-derived rejection classifiers PCA input variables and the PC scores are shown as factor maps in (A) PC2 vs PC1 and (B) PC2 vs PC3. ABMR-related classifiers include g_{Prob} – g > 0 classifier; ptc_{Prob} – ptc > 0 classifier, and $ABMR_{Prob}$ – ABMR classifier. TCMR-related classifiers include t_{Prob} – t > 1 classifier, i_{Prob} – i > 1 classifier, and $TCMR_{Prob}$ – TCMR classifier. PCAs for biopsies are shown in (C) PC2 vs PC1 and (D) PC2 vs PC3. (E) UMAP visualization of the 3230 population with variation compressed into 2 dimensions only. PCAs and UMAP panels are colored by the 7-archetype rejection model cluster assignments (no rejection, TCMR1, TCMR2, TCMR/Mixed, Minor, EABMR, and FABMR). ABMR, antibody-mediated rejection; EABMR, early-stage antibody-mediated rejection; FABMR, fully developed antibody-mediated rejection; NR, No rejection; TCMR, T cell–mediated rejection.

Note that in PCA and UMAP, although we use archetypal clustering to group the biopsies for treatment decisions, the rejection molecular changes are continuous and lack true separation.

3.3. Features of the rejection archetype groups

The relationship of these new scores to molecular and clinical findings in INTERHEART biopsies with complete phenotyping is shown in Table 1 (more details in Supplementary Table 6). Biopsies classified as NR (48% of biopsies) had low mean scores for all molecular abnormalities, low donor-specific antibody (DSA) positivity, high expression of normal heart transcripts, and good function (LVEF). Biopsies with Minor rejection (24% of biopsies) also had high expression of normal heart transcripts and good function (increased LVEF) and were similar to the NR group for recent injury (cardiac injury transcripts [cIRITs]) but had mild increases in DSA and in scores for molecular features of ABMR and TCMR. Thus, low-level molecular rejection was operating below the threshold established for TCMR and ABMR in about a quarter of all biopsies with minimal parenchymal effects.

All TCMR archetypes (TCMR1, TCMR2, and TCMR/Mixed) had elevated TCMR features, including transcript sets reflecting T cell burden, cytotoxic T cells, interferon gamma-inducible transcripts, and macrophages. They also had increased transcripts reflecting recent injury, depressed expression of normal heart transcripts, and lower LVEF. TCMR1 was earlier and more intense than TCMR2 (median 330 vs 660 days), but TCMR2 had more fibrosis and lower LVEF. TCMR biopsies had high scores for the LoLVEF-$_{Prob}$ classifier (0.41-0.48) compared with other groups (0.17-0.23).

ABMR was often positive for DSA and had higher expression of ABMR-related transcript sets eg, DSA-selective, natural killer

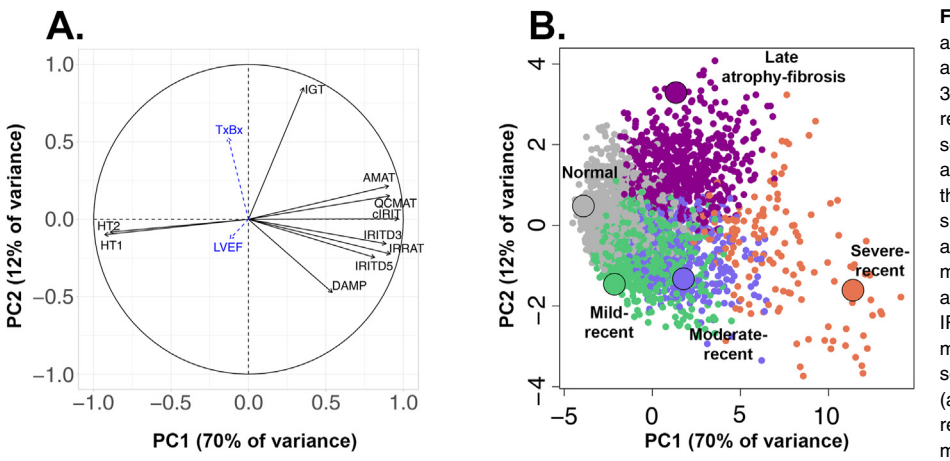

Figure 3. Principal component analysis (PCA) and archetypal analysis using 10 atrophy fibrosis–related and recent injury-related transcript set scores in the 3230 heart transplant biopsy population. (A) The correlations (vectors) between the 10 transcript set scores and the PC scores are shown in PC2 vs PC1 as factor maps. TxBx and LVEF are in dashed blue as they are not included as input in the PCA. (B) PCA is shown as PC2 vs PC1 for biopsies, colored by the 5-archetype injury model group assignments (normal, mild-recent, moderate-recent, severe-recent, and late atrophy-fibrosis). Injury-related transcript set scores: IRITD3, injury and rejection–induced transcript (intermediate); IRITD5, injury and rejection–induced transcript (late); IRRAT, injury/repair-associated transcript (acute kidney injury); cIRIT, cardiac injury and repair–induced transcript; DAMP, damage-associated molecular pattern transcript; HT1, heart transcript set 1; HT2, heart transcript set 2. Atrophy fibrosis–related transcript set scores: QCMAT, quantitative constitutive macrophage-associated transcript; AMAT, alternative macrophage-associated transcript; IGT, immunoglobulin transcript. LVEF, left ventricular ejection fraction; TxBx, time of biopsy posttransplant.

cell–expressed, interferon gamma-inducible, and ABMR-associated transcripts. EABMR was earlier than fully developed (FABMR, median 266 vs 1328 days), but FABMR was more intense. ABMR was better tolerated than TCMR, with higher LVEF, lower $LoLVEF_{Prob}$ scores, and less molecular injury (cIRITs).

TCMR/mixed was often positive for DSA (78%) and had features of both ABMR and TCMR, with increased molecular injury (cIRITs) and reduced normal heart transcripts and function.

3.4. Comparing new rejection archetypes with histology

Table 2 compares histologic diagnoses with the rejection archetype diagnoses in 1435 biopsies with histologic assessment recorded. As in previous analyses,[8] International Society for Heart and Lung Transplantation-based histology diagnoses recorded by each center were simplified to permit comparisons. Histology diagnosed 198 biopsies with rejection: 121 TCMR and 77 ABMR. Molecular analysis designated 333 biopsies with rejection archetypes: 113 TCMR and 220 ABMR. Thus, there was more molecular ABMR than histologic ABMR. Of 178 biopsies with definite histologic rejection, 87 (44%) had definite molecular rejection.

In 639 histologic NR biopsies, many were designated molecularly as NR (454), some as Minor or ABMR, but rarely as TCMR. In 121 histologic TCMR biopsies, only 25 had molecular TCMR although some were Minor (29) or mixed (8). Many were molecular NR (40) or ABMR (19). Histologic mixed (n = 17) was rarely molecular-mixed archetype (only 1).

The 77 histologic ABMR biopsies were often designated molecular ABMR (31) or Minor (23) archetypes, but none were TCMR. The 426 histologic probable TCMR was often NR (213) or Minor (117), but 70 had molecular ABMR. The 155 histologic probable ABMR was often molecular ABMR (48) or Minor (45).

3.5. Updating the injury archetypes

All 3230 biopsies were given scores for 10 injury-related transcript sets reflecting acute or chronic parenchymal injury.[5] In PCA, the vectors for all injury scores correlated with PC1, whereas PC2 separated recent injury (negative) from atrophy-fibrosis (positive, a condition in all transplants involving irreversible loss of parenchymal cells [atrophy] accompanied by matrix remodeling and accumulation of collagen [fibrosis]) (Fig. 3A). Time of biopsy posttransplant (TxBx) correlated strongly with PC2, and LVEF correlated negatively with PC1 and PC2.

The injury archetype groups were similar to the earlier model[5]: 1141 minimal injury or "Normal" (35%); 794 Mild-recent (25%), 525 Moderate-recent (16%), and 149 Severe-recent (5%); and 621 Late atrophy-fibrosis (19%) groups. PC1 separated all groups from normal and PC2 separated Late atrophy-fibrosis (positive) from recent injury groups (negative, Fig. 3B).

Sorting all 3230 biopsies by TxBx, the recent injury groups were earliest, followed by normal, then by emergence of late atrophy-fibrosis groups (Table 3, more data in Supplementary Table 7). Recent injury-related transcripts, such as cIRITs (derived in mouse heart isografts), macrophage transcripts, and normal heart transcripts were most abnormal in Severe-recent injury. Atrophy fibrosis–related transcripts (immunoglobulin transcripts) were highest in the Late atrophy-fibrosis group. TCMR features increased in Severe-recent injury and Late atrophy-fibrosis groups and ABMR features in the Late atrophy-fibrosis group.

Function was most abnormal in Severe-recent injury (mean LVEF, 56%) and Late atrophy-fibrosis (mean LVEF, 55%) groups than that in Normal, Mild-recent, and Moderate-recent groups (all mean values, >60%). The $LoLVEF_{Prob}$ classifier score showed similar patterns. Although numerical differences in mean LVEF

Table 3
Features of the 5 injury archetype groups in all 3230 biopsies.

Biopsy groups	Feature	Normal	Mild-recent	Moderate-recent	Severe-recent	Late atrophy-fibrosis
	n (%)	1141 (35.3)	794 (24.6)	525 (16.3)	149 (4.6)	621 (19)
	Days posttransplant (median)	454	143	119	65[a]	1523[b]
	Days posttransplant (mean)	1359	579	806	533[a]	2083[b]
Macrophage transcripts (QCMATs)		0.68[a]	0.90	1.02	2.06[b,c]	1.29
Normal heart transcripts (HTs)		0.86[a]	0.85	0.73	0.33[b,c]	0.69
Recent injury-induced transcripts (cIRIT)		0.78[a]	0.84	0.98	1.31[b,c]	0.98
Immunoglobulin transcripts (IGTs)		0.81	0.77	0.74[a]	1.36	2.50[b,c]
Function-related	LVEF	61	63[b]	63[b]	56	55[a,b]
	Fraction with low LVEF $\leq$ 55	0.20	0.12[a]	0.16	0.35	0.39[b,c]
	Classifier score $LoLVEF_{Prob}$	0.18	0.13[a]	0.15	0.35[b,c]	0.32

ABMR, antibody-mediated rejection; LVEF, left ventricular ejection fraction; $LoLVEF_{Prob}$, low left ventricular ejection fraction–previously published; TCMR, T cell–mediated rejection.

[a] The lowest per row.

[b] The highest per row.

[c] The most abnormal (compared with normal) values per row.

may not seem clinically relevant per se, these low LVEF groups contain many cases with clinically relevant dysfunction.

3.6. Injury archetypes in NR biopsies

The features of the injury groups in 1564 biopsies designated as NR archetype were similar to those in all biopsies (Table 4, complete details in Supplementary Table 8), supporting the independence of the rejection and injury assessments. Among NR biopsies, the recent injury groups were the earliest followed by Normal, and the Late atrophy-fibrosis groups were the most late. Removing rejection biopsies greatly reduced the number of Severe-recent injury and Late atrophy fibrosis, reflecting the close association of those injury states with rejection.

3.7. Relating rejection and injury states to TxBx

TxBx was strongly associated with the probability of assignment of each rejection archetype (Fig. 4A, B; Fig. 4B with the NR curve removed to show more detail in the rejection groups). NR scores were most frequent early then fell progressively. TCMR1 and TCMR2 archetype biopsies peaked in frequency in the second year and then decreased. TCMR/Mixed plateaued after 3 years and was sustained. There was some EABMRs, probably

Table 4
Features in the 5 injury archetype groups in 1564 biopsies classified as no rejection.

Biopsy groups	Feature	Normal	Mild-recent	Moderate-recent	Severe-recent	Late atrophy-fibrosis
	n (%)	723 (46)	456 (29)	231 (14.7)	45 (2.8)	109 (6.9)
	Days posttransplant (median)	365	11[a]	46	29	1674[b]
	Days posttransplant (mean)	1212	567	338	234[a]	2058[b]
Macrophage transcripts (QCMATs)		0.60[a]	0.82	0.91	2.08[b,c]	1.01
Normal heart transcripts (HTs)		0.88[b]	0.87	0.73	0.19[a,c]	0.76
Recent injury-induced transcripts (cIRIT)		0.76	0.82	0.97	1.42[b,c]	0.90
Immunoglobulin transcripts (IGTs)		0.76	0.68	0.57[a]	0.79	2.43[b,c]
Function-related	LVEF	61	61	63[b]	56[a,c]	56[a,c]
	Fraction with low LVEF $\leq$ 55	0.21	0.16	0.12[a]	0.27	0.30[b,c]
	Classifier score $LoLVEF_{Prob}$	0.17	0.13[a]	0.17	0.27	0.32[b,c]

ABMR, antibody-mediated rejection; LVEF, left ventricular ejection fraction; $LoLVEF_{Prob}$, low left ventricular ejection fraction–previously published; TCMR, T cell–mediated rejection.

[a] The lowest per row.

[b] The highest per row.

[c] The most abnormal (compared with normal) values per row.

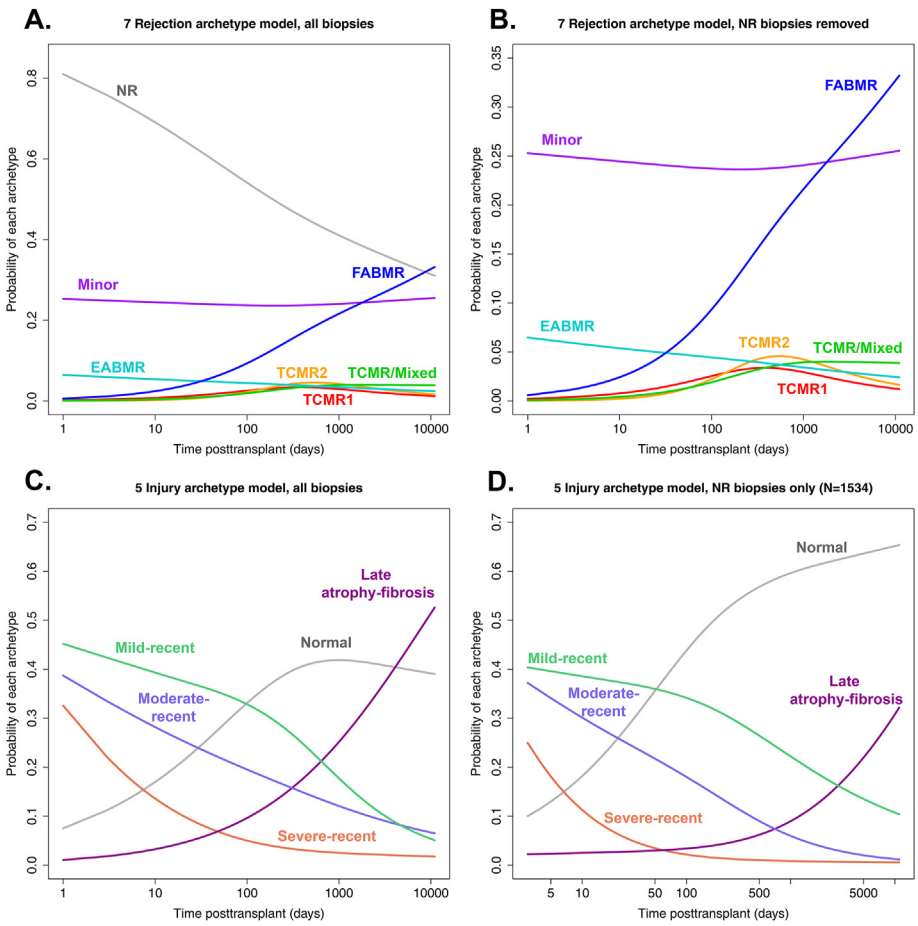

Figure 4. Relationships of the rejection and injury archetypal analysis classes to time posttransplant. (A) Probabilities of assignment to each rejection archetype cluster are shown as smoothed splines over time posttransplant. (B) The same results as panel A but removing the NR group to show more detail in the rejection groups. (C) Probability of assignment to each injury archetype cluster shown as smoothed splines over time. (D) The same results as panel C but only including biopsies assigned to the NR archetype group. NR, No rejection.

reflecting presensitized patients. The FABMR archetype rose in frequency after 100 days and was dominant late. Minor biopsies were found relatively consistently across all periods.

Severe-recent, Moderate-recent, and Mild-recent groups were most frequent early, likely reflecting the acute injury presumably induced by donation-preservation-implantation and its resolution with time (Fig. 4C). Normal biopsies were uncommon early but rose to plateau after about 1 year. Late atrophy-fibrosis accelerated steadily upward after 1 year.

Figure 4D shows that the time-injury relationship in the 1564 NR archetype biopsies was similar to that in the whole 3230 biopsy population.

3.8. Rejection-injury relationships

We examined the injury states associated with each rejection state, grouping all biopsies by their rejection state (rows) and injury state (columns, Table 5). By rows, most biopsies with NR or Minor rejection had normal parenchyma or Mild- to Moderate-recent injury. In contrast, TCMR (including mixed) almost always had extensive parenchymal damage—Severe-recent injury (45/149) or Late atrophy- fibrosis (109/621)—and rarely had normal parenchyma. TCMR1 biopsies were often called Severe-recent injury by archetypes (45%); TCMR2 and TCMR/Mixed biopsies were predominantly called atrophy-fibrosis (74% and 70%, respectively). ABMR was better tolerated than TCMR, rarely called Severe-recent injury (5%), but 37% of ABMR had Late atrophy-fibrosis.

3.9. Survival postbiopsy

Figure 5 shows the actuarial curves for the rejection and injury archetype groups and histology diagnosis groups. (One random biopsy per transplant, results similar using the last biopsy per patient—data not shown.) The rejection archetypes (Fig. 5A) were dominated by poor survival after TCMR1 biopsies and good survival after FABMR biopsies (model $P = 7 \times 10^{-5}$). Figure 5B shows the actuarial 3-year analysis for the injury archetypes, with reduced survival in the Severe-recent and Late atrophy-fibrosis groups (model $P = 5 \times 10^{-5}$). Figure 5C shows survival by injury group within the 1564 NR archetype (model $P = .01$), with increased losses in Severe-recent and Late atrophy-fibrosis groups. Figure 5D illustrates survival per histology diagnostic groups (insignificant, model $P = 1.0$).

4. Discussion

The goal of this study was to create a new molecular rejection classification independent of the assessment of parenchymal injury by eliminating the cross-reactions with acute injury that we observed in the first-generation RAT-based rejection classification.[3] To increase the power of the machine learning algorithms,

Table 5
Classifying each biopsy by its rejection archetype (rows) and its injury archetype (columns): number of biopsies in each rejection+injury subgroup (% by row).

Rejection archetypal analytic classes	Injury archetype classes, n (%)					Row total
	Normal	Mild-recent	Moderate-recent	Severe-recent	Late atrophy-fibrosis	
No rejection[a]	723 (46)[b]	456 (29)[b]	231 (15)	45 (3)	109 (7)	1564
Minor[a]	287 (37)[b]	242 (31)[b]	118 (15)	16 (2)	114 (15)	777
All TCMR (including mixed)[a]	13 (5)	10 (4)	10 (4)	55 (22)[b]	163 (65)[b]	251
TCMR1[c]	1 (1)	4 (5)	0 (0)	34 (45)	36 (48)	75
TCMR2[c]	7 (8)	4 (5)	5 (6)	7 (8)	65 (74)	88
TCMR/mixed[c]	5 (6)	2 (2)	5 (6)	14 (16)	62 (70)	88
All ABMR[a]	118 (18)	86 (13)	166 (26)[b]	33 (5)	235 (37)[b]	638
EABMR[c]	18 (14)	35 (28)	24 (19)	11 (9)	39 (31)	127
FABMR[c]	100 (20)	51 (10)	142 (28)	22 (4)	196 (38)	511
Column total	1141	794	525	149	621	3230

ABMR, antibody-mediated rejection; EABMR, early-stage antibody-mediated rejection; FABMR, fully-developed antibody-mediated rejection; TCMR, T cell–mediated rejection.

[a] Main rejection groups: no rejection, minor, all TCMR, and all ABMR.

[b] The 2 largest rejection+injury classes within each rejection class row.

[c] Subgroups.

we expanded the reference set to 3230 biopsies by combining clinical trial biopsies with service biopsies. As we had hypothesized, the use of rejection classifiers produced a PCA and archetypal system unrelated to early injury, with no acute injury relationship with PC3 and no acute injury archetype assigned. Rejection archetypes classified the 3230 biopsies as 8% TCMR, 20% ABMR, and 24% with Minor rejection activity, reflecting subthreshold increases in ABMR and TCMR features and increased DSA positivity in biopsies ordinarily considered as NR and with no immediate parenchymal injury (eg, in the cIRITs). When we compared the new rejection classes with the injury archetype classes, TCMR was strongly associated with severe parenchymal injury but ABMR rarely had severe injury and instead often had Late atrophy-fibrosis, indicating long-term risk. Both rejection and injury archetypes were associated with increased risk of short-term failure, with the lowest survival in TCMR1 and in severe injury and Late atrophy-fibrosis archetypes, even those without rejection.

TxBx significantly correlated with the frequency of TCMR and ABMR, similar to the timing of rejection states in kidney transplants.[10] The TCMR archetypes showed progression in median time posttransplant: TCMR1, 360 days; TCMR2, 660 days; and TCMR/Mixed, 938 days, suggesting a long-term evolution that peaked and then declined. TCMR1 was the most intense, whereas TCMR2 and TCMR/Mixed were less intense but showed more atrophy fibrosis. The decline in TCMR activity in the population after 3 years probably reflects regulatory mechanisms in the host cognate T cell response.[23] ABMR archetypes evolved from EABMR (median 266 days) to FABMR (median 1328 days). However, unlike TCMR, ABMR became more intense over time: scores relating to ABMR activity and DSA positivity increased from NR to Minor to EABMR to FABMR. These findings in the biopsied population are compatible with the natural history of the cognate immune response, with an earlier rise and subsequent fall of TCMR activity and later maturation of the host antibody response and its consequence as sustained ABMR activity.

Although not the main subject of this analysis, histology-molecular archetype relationships as in earlier analyses[16] showed more agreement for NR and ABMR than for TCMR. Given that rejection operates as gradients without clear boundaries between groups, discrepancies among rejection classifications are expected. The agreement between histologic and molecular TCMR (21%) is similar to the κ value for the agreement among pathologists on acute cellular rejection in the CARGO II study[24] (0.28), suggesting that a major factor in histology-molecular discrepancies is the "noise" in histology imposed by interobserver disagreement. The same pattern has been seen in kidneys, where there is also considerable disagreement among pathologists for TCMR.[25,26] However, MMDx assessments can also be affected by the relatively small sample size imposed in the ClinicalTrials.gov environment, where institutional review boards severely restrict tissue availability, increasing concerns about sampling error and quilty effects. Nevertheless, the associations of molecular TCMR with molecular injury, depressed LVEF, and risk of graft loss suggest that the molecular rejection assessments are largely correct.

This study lacked the resources for central review by an expert panel, and we are seeking to define the relationship between MMDx and expert central panel review in future studies. In addition, we acknowledge that, although our FABMR group had good survival, some studies have noted an association between

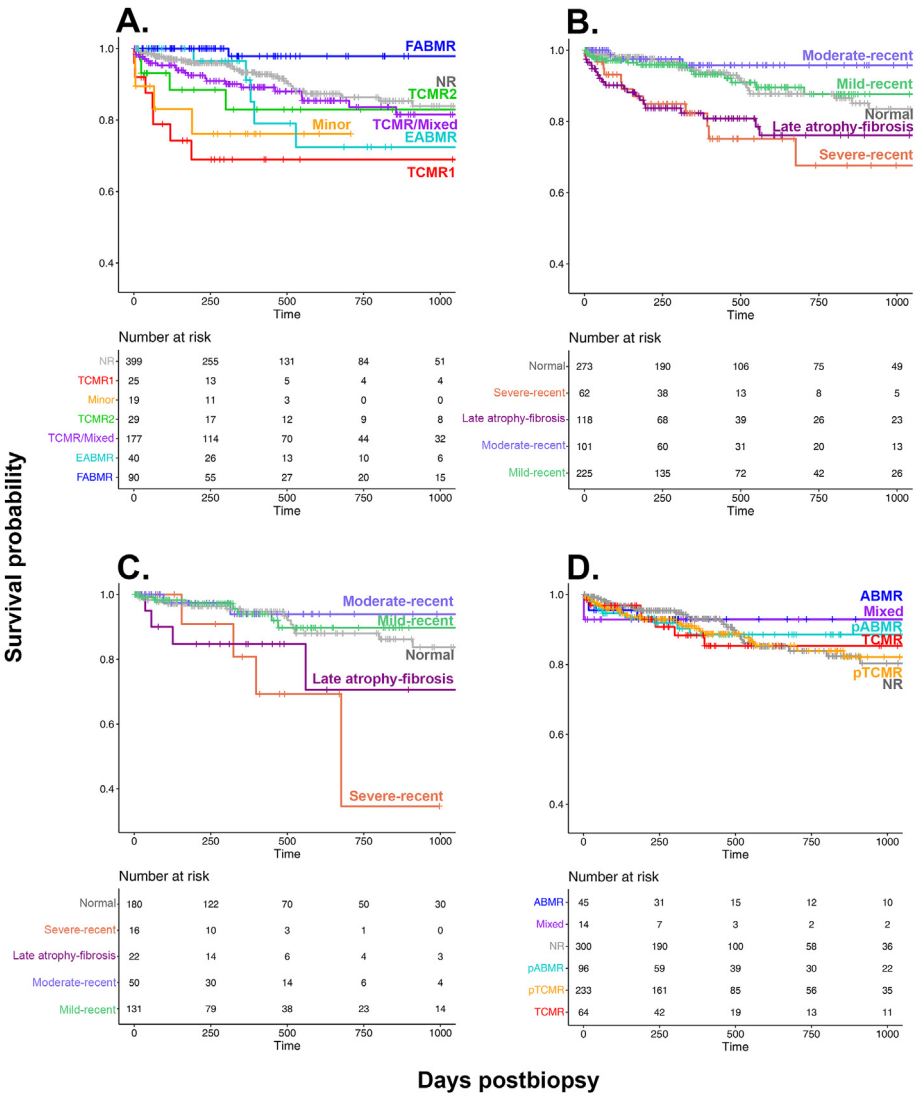

Figure 5. Survival probability within rejection archetypes, injury archetypes, or histology diagnoses. Kaplan-Meier plots showing 3-year postbiopsy survival stratified by rejection archetype groups (A), injury archetype groups (B), injury archetype groups in No rejection only (C), and histology diagnosis groups (D). All biopsy counts (n) per panel represent 1 random biopsy per patient within the selected population.

histologic ABMR and cardiovascular-related mortality[27] but in population-based studies with longer time frames that differ from the present cross-sectional biopsy-based study. The strong association of FABMR with Late atrophy-fibrosis suggests that our FABMR cases may also show risk of graft failure in long-term studies.

As expected, the large Late atrophy-fibrosis group (19% of all biopsies) overlaps the features expected for cardiac allograft vasculopathy (CAV). Late atrophy-fibrosis had a median of 1523 days, with dysfunction (fraction with low LVEF, 39%), increased risk of failure, and strong associations with rejection.[28] CAV shares features with this state and is itself a diffuse microcirculation process.[29] Because standard-of-care CAV assessment was not generally available in INTERHEART at the time of biopsy, new studies will be needed to define the relationship between the CAV phenotype and the biopsy-based Late atrophy-fibrosis phenotype.

This study has the limitations of all cross-sectional biopsy studies, including limited long-term follow-up data for survival estimates. Moreover, all biopsy studies underrepresent the best transplants that never get indication biopsies, imposing constraints on the generalization of the conclusions to all heart transplants. Postrejection survival curves in this study were not intended to be used as general survival prediction models. The relationship between early molecular injury states and formal assignment of primary graft dysfunction (PGD) was not assessed because the PGD status was not assigned in all centers. However, many early biopsies had various degrees of parenchymal injury, and future work will examine whether these biopsies have PGD. Our actual data indicate that early dysfunction is more a spectrum than a discrete state, but the PGD status would be of interest.

One of the major findings in the new rejection archetypes is smoldering ABMR and/or TCMR activity in the 24% of hearts with minor rejection, indicating that rejection activity is less well-

controlled by the current immunosuppressive drugs than previously believed. Although the minor biopsies differed little from the NR biopsies in injury, function, and outcomes, such activity could have long-term risks not captured in a cross-sectional study.

Our focus on understanding rejection-injury interactions should not distract us from trying to reduce nonimmune injury. Much of the Mild-recent, Moderate-recent, and Severe-recent injury was early when rejection is uncommon and presumably related to the donation-preservation-implantation period. This early cardiomyocyte injury likely contributes to long-term injury, dysfunction, and increased risk of graft loss. All stressors—brain death, ischemia, rejection, and others—ultimately operate to produce impaired function and failure through their effects on the parenchyma. Whether injury also induces rejection is unknown: this has long been suspected but never proven. Being able to quantitatively measure parenchymal injury puts us in a position to evaluate new management options of the universal burden of brain death and other stresses on heart transplants. Furthermore, when considering the "effect of treatment of rejection" questions, we can now assess the effect on rejection and parenchymal injury separately, helping to distinguish between incomplete treatment, recurrence of rejection posttreatment, rejection progression, or legacy of cardiomyocyte injury.

Acknowledgments

The authors thank Jeff Reeve and Jessica Chang for analyzing the data and Martina Mackova and Anna Hutton for processing biopsy samples.

Funding

This research has been principally supported by grants from Genome Canada, Canada Foundation for Innovation, the University of Alberta Hospital Foundation, the Alberta Ministry of Advanced Education and Technology, the Mendez National Institute of Transplantation Foundation, and Industrial Research Assistance Program. Partial support was also provided by funding from a licensing agreement with the One Lambda division of Thermo Fisher. Some biopsies were provided by Dr. Alexandre Loupy, Paris, France.

Author contributions

P.F.H. was the principal investigator and wrote and reviewed the manuscript. K.M.T. wrote and reviewed the manuscript. A.Z.A.-Z., M.C., M.G.C.-L., E.C.D., M.D., J.G., S.H., A.J., D.H.K., J.K., P.M., V.M., J.P., L.P., K.S., J.S., and A.Z. collected biopsy samples and reviewed the manuscript.

Declaration of competing interest

The authors of this manuscript have conflicts of interest to disclose as described by the *American Journal of Transplantation*: P.F. Halloran held a Canada Research Chair in Transplant Immunology until 2008 and currently holds the Muttart Chair in Clinical Immunology; holds shares in Transcriptome Sciences (TSI), a University of Alberta research company dedicated to developing molecular diagnostics, supported in part by a licensing agreement between TSI and Thermo Fisher Scientific, and by a research grant from Natera; and is a consultant to Natera. The other authors of this manuscript have no conflicts of interest to disclose as described by the American Journal of Transplantation.

Data availability statement

The.CEL files are available at Gene Expression Omnibus (GSE262742).

Appendix A. Supplementary data

Supplementary data to this article can be found online at https://doi.org/10.1016/j.ajt.2024.03.031.

ORCiD

Philip F. Halloran https://orcid.org/0000-0003-1371-1947
Katelynn Madill-Thomsen https://orcid.org/0000-0003-2781-6934
Arezu Z. Aliabadi-Zuckermann https://orcid.org/0000-0002-2808-7158
Martin Cadeiras https://orcid.org/0000-0003-4545-2871
Marisa G. Crespo-Leiro https://orcid.org/0000-0002-3085-167X
Eugene C. Depasquale https://orcid.org/0000-0002-0638-5218
Johannes Gökler https://orcid.org/0000-0003-4509-2482
Shelley Hall https://orcid.org/0000-0002-4894-396X
Aayla Jamil https://orcid.org/0000-0001-9471-3383
Jon Kobashigawa https://orcid.org/0000-0001-9308-3172
Peter Macdonald https://orcid.org/0000-0001-5378-2825
Vojtech Melenovsky https://orcid.org/0000-0001-8921-7078
Luciano Potena https://orcid.org/0000-0001-7388-5012
Josef Stehlik https://orcid.org/0000-0002-7362-0513
Andreas Zuckermann https://orcid.org/0000-0002-8054-8150

References

1. Stehlik J, Kobashigawa J, Hunt SA, Reichenspurner H, Kirklin JK. Honoring 50 years of clinical heart transplantation in circulation: in-depth state-of-the-art review. *Circulation*. 2018;137(1):71–87.
2. Nikolova AP, Kobashigawa JA. Cardiac allograft vasculopathy: the enduring enemy of cardiac transplantation. *Transplantation*. 2019;103(7):1338–1348.
3. Reeve J, Kim DH, Crespo-Leiro MG, et al. Molecular diagnosis of rejection phenotypes in 889 heart transplant biopsies: the INTERHEART study. *J Heart Lung Transplant*. 2018;37(4):S27.
4. Halloran PF, Reeve J, Aliabadi AZ, et al. Exploring the cardiac response to injury in heart transplant biopsies. *JCI Insight*. 2018;3(20):e123674.
5. Madill-Thomsen KS, Reeve J, Aliabadi-Zuckermann A, et al. Assessing the relationship between molecular rejection and parenchymal injury in heart transplant biopsies. *Transplantation*. 2022;106(11):2205–2216.
6. Parkes MD, Aliabadi AZ, Cadeiras M, et al. An integrated molecular diagnostic report for heart transplant biopsies using an ensemble of diagnostic algorithms. *J Heart Lung Transplant*. 2019;38(6):636–646.
7. Halloran PF, Potena L, Van Huyen JD, et al. Building a tissue-based molecular diagnostic system in heart transplant rejection: the heart Molecular Microscope Diagnostic (MMDx) System. *J Heart Lung Transplant*. 2017;36(11):1192–1200.
8. Halloran PF, Madill-Thomsen KS, Aliabadi-Zuckermann AZ, et al. Many heart transplant biopsies currently diagnosed as no rejection have mild molecular antibody-mediated rejection-related changes. *J Heart Lung Transplant*. 2022;41(3):334–344.

9. Halloran PF, Madill-Thomsen K, Mackova M, et al. Molecular states associated with dysfunction and graft loss in heart transplants. *J Heart Lung Transplant*. 2024;43(3):508–518. https://doi.org/10.1016/j.healun.2023.11.013.
10. Reeve J, Bohmig GA, Eskandary F, et al. Assessing rejection-related disease in kidney transplant biopsies based on archetypal analysis of molecular phenotypes. *JCI Insight*. 2017;2(12):e94197.
11. Billingham M, Kobashigawa JA. The revised ISHLT heart biopsy grading scale. *J Heart Lung Transplant*. 2005;24(11):1709.
12. Berry GJ, Burke MM, Andersen C, et al. The 2013 International Society for Heart and Lung Transplantation Working Formulation for the standardization of nomenclature in the pathologic diagnosis of antibody-mediated rejection in heart transplantation. *J Heart Lung Transplant*. 2013;32(12):1147–1162.
13. Colvin MM, Cook JL, Chang P, et al. Antibody-mediated rejection in cardiac transplantation: emerging knowledge in diagnosis and management: a scientific statement from the American Heart Association. *Circulation*. 2015;131(18):1608–1639.
14. Loupy A, Duong Van Huyen JP, Hidalgo LG, et al. Gene expression profiling for the identification and classification of antibody-mediated heart rejection. *Circulation*. 2017;135(10):917–935.
15. Halloran PF, Reeve J, Akalin E, et al. Real time central assessment of kidney transplant indication biopsies by microarrays: the INTERCOMEX study. *Am J Transplant*. 2017;17(11):2851–2862.
16. Halloran PF, Madill-Thomsen KS. The molecular microscope diagnostic system: assessment of rejection and injury in heart transplant biopsies. *Transplantation*. 2023;107(1):27–44.
17. Ritchie ME, Phipson B, Wu D, et al. limma powers differential expression analyses for RNA-sequencing and microarray studies. *Nucleic Acids Res*. 2015;43(7):e47.
18. R: A language and environment for statistical computing. R Foundation for statistical Computing. http://www.r-project.org/. Published 2019. Updated 2019.
19. Lê S, Josse J, Husson F. FactoMineR: an R package for multivariate analysis. *J Stat Softw*. 2008;25(1):18.
20. Eugster MJA, Leisch F. From spider-man to hero—archetypal analysis in R. *J Stat Softw*. 2009;30(8):1–23.
21. Harrell Jr FE. rms: regression modeling strategies. *R package version 6.7-1*; 2023. https://CRAN.R-project.org/package=rms.
22. Harrell Jr FE, Dupont C. Hmisc: Harrell Miscellaneous. *R package version 4.3-0*; 2019. https://CRAN.R-project.org/package=Hmisc. Published.
23. Halloran PF, Chang J, Famulski K, et al. Disappearance of T cell-mediated rejection despite continued antibody-mediated rejection in late kidney transplant recipients. *J Am Soc Nephrol*. 2015;26(7):1711–1720.
24. Crespo-Leiro MG, Zuckermann A, Bara C, et al. Concordance among pathologists in the second Cardiac Allograft Rejection Gene Expression Observational Study (CARGO II). *Transplantation*. 2012;94(11):1172–1177.
25. Furness PN, Taub N, Assmann KJ, et al. International variation in histologic grading is large, and persistent feedback does not improve reproducibility. *Am J Surg Pathol*. 2003;27(6):805–810.
26. Reeve J, Sellares J, Mengel M, et al. Molecular diagnosis of T cell-mediated rejection in human kidney transplant biopsies. *Am J Transplant*. 2013;13(3):645–655.
27. Kfoury AG, Renlund DG, Snow GL, et al. A clinical correlation study of severity of antibody-mediated rejection and cardiovascular mortality in heart transplantation. *J Heart Lung Transplant*. 2009;28(1):51–57.
28. Loupy A, Coutance G, Bonnet G, et al. Identification and characterization of trajectories of cardiac allograft vasculopathy after heart transplantation: a population-based study. *Circulation*. 2020;141(24):1954–1967.
29. Daud A, Xu D, Revelo MP, et al. Microvascular loss and diastolic dysfunction in severe symptomatic cardiac allograft vasculopathy. *Circ Heart Fail*. 2018;11(8):e004759.